Physiological and histopathological responses following closed rotational head injury depend on direction of head motion

Published in final edited form as:
Exp Neurol. 2011 January ; 227(1): 79–88. doi:10.1016/j.expneurol.2010.09.015.

Physiological and histopathological responses following closed rotational head injury depend on direction of head motion

Stephanie A. Eucker[a], **Colin Smith**[b], **Jill Ralston**[a], **Stuart H. Friess**[c], and **Susan S. Margulies**[a]

[a] Department of Bioengineering, School of Engineering and Applied Science, University of Pennsylvania, Philadelphia, PA, USA

[b] Department of Pathology, University of Edinburgh, Edinburgh, Scotland, UK

[c] Department of Anesthesiology and Critical Care Medicine, The Children's Hospital of Philadelphia, Philadelphia, PA, USA

Abstract

Rotational inertial forces are thought to be the underlying mechanism for most severe brain injuries. However, little is known about the effect of head rotation direction on injury outcomes, particularly in the pediatric population. Neonatal piglets were subjected to a single non-impact head rotation in the horizontal, coronal, or sagittal direction, and physiological and histopathological responses were observed. Sagittal rotation produced the longest duration of unconsciousness, highest incidence of apnea, and largest intracranial pressure increase, while coronal rotation produced little change, and horizontal rotation produced intermediate and variable derangements. Significant cerebral blood flow reductions were observed following sagittal but not coronal or horizontal injury compared to sham. Subarachnoid hemorrhage, ischemia, and brainstem pathology were observed in the sagittal and horizontal groups but not in a single coronal animal. Significant axonal injury occurred following both horizontal and sagittal rotations. For both groups, the distribution of injury was greater in the frontal and parietotemporal lobes than in the occipital lobes, frequently occurred in the absence of ischemia, and did not correlate with regional cerebral blood flow reductions. We postulate that these direction-dependent differences in injury outcomes are due to differences in tissue mechanical loading produced during head rotation.

Keywords

animal models; brain ischemia; brain trauma; cerebral blood flow; neuropathology; subarachnoid hemorrhage

Corresponding author: Susan S. Margulies, Address: Department of Bioengineering, School of Engineering and Applied Science, University of Pennsylvania, 240 Skirkanich Hall, 210 S. 33rd Street, Philadelphia, PA 19104, USA, Phone: +1 215-898-0882, Fax: +1 215-573-2071, margulie@seas.upenn.edu.

Disclosure/Conflict of Interest: The authors declare no conflict of interest.

1. Introduction

Traumatic brain injury (TBI) is a leading cause of death and disability in infants in the U.S. (Langlois, et al., 2004). These patients may present with irritability, seizures, loss of consciousness, and respiratory difficulties (Gruskin and Schutzman, 1999, Johnson, et al., 1995). Increased intracranial pressure (ICP) and decreased cerebral blood flow (CBF) are frequently observed (Adelson, et al., 1997, Sharples, et al., 1995). Radiological and pathological findings include subdural, subarachnoid and parenchymal hemorrhages, skull fractures, diffuse brain swelling, axonal injury, and ischemia (Duhaime, et al., 1992, Geddes, et al., 2001). However, the mechanisms of injury are incompletely understood, and effective treatment is limited, particularly for severely injured patients.

The relative importance of primary versus secondary injuries on TBI outcomes in infants has been hotly debated. Primary injury refers to the physical derangements, such as tissue deformation and tissue failure, that occur during the traumatic event; it is highly dependent on the specific mechanical loading conditions to the head (Ommaya, 1985). For instance, head impact frequently produces focal contusions, whereas non-impact rotational head motion has been shown to produce more diffuse brain injuries (Adams, et al., 1985, Gennarelli, et al., 1982, Ommaya, 1985). Furthermore, falls are the most common cause of mild to moderate TBI in infants, whereas motor vehicle crashes and assault, which have a larger rotational component, more frequently produce severe or fatal TBI, suggesting the importance of rotational head motion in the most severe brain injuries (Arbogast, et al., 2005, Duhaime, et al., 1992). Direction of head motion may also be an important factor in TBI outcomes, and would therefore need to be considered when developing safety standards for automobiles and helmets. Limited studies in adult pigs and primates have demonstrated distinct physiological and histopathological responses to head rotations in different directions, likely due to brain geometry asymmetries among the different axes (Gennarelli, et al., 1982, Gennarelli, et al., 1987, Smith, et al., 2000). The effect of rotation direction in the pediatric population remains to be examined.

Secondary injury encompasses the array of biological responses to the initial traumatic event that have been observed, including ion channel dysfunction, excitotoxicity, ischemia, and derangements in CBF and blood pressure (Bayir, et al., 2003, Kochanek, et al., 2000). These changes can continue to develop for days following the initial traumatic event and can be monitored clinically; thus, they are potential targets for therapeutic intervention (Bayir, et al., 2003). However, targeted therapy at a single injury mechanism has been of limited clinical success, and it is likely that optimal treatment must take multiple mechanisms into consideration (Kochanek, et al., 2000). In particular, the coupled interaction between the primary mechanical insult and the initiation of secondary insults, such as CBF changes and ischemia, requires further investigation.

We have previously developed a horizontal rotational brain injury model in neonatal piglets that recapitulates many of the clinical findings observed in infant TBI (Raghupathi and Margulies, 2002). However, the effects of rotation in the sagittal and coronal directions are unknown. We hypothesize that head rotation direction affects immediate post-injury physiological responses, including regional cerebral blood flow changes, unconsciousness times, and incidences of apnea, as well as early pathological outcomes including regional axonal and ischemic injuries immediately following rotational closed head injury in piglets. In addition, we identify the importance of early cerebral blood flow reductions on the initial post-injury development of both axonal injury and tissue infarction.

2. Material and methods

2.1. Animal preparation

All protocols were approved by the Institutional Animal Care and Use Committee of the University of Pennsylvania. Thirty-six neonatal (3-5 day old) piglets, whose level of brain development and myelination correspond to that of human infants 1-3 months old (Armstead, 2005), were used for this study. Vital signs including heart rate, arterial oxygen saturation (SaO_2), and end tidal CO_2 were recorded for the duration for each study. Supplemental oxygen and mechanical ventilator support were adjusted as needed to maintain normoxia and normocarbia. Rectal temperature was maintained between 37-39°C using a heating pad and lamp.

Piglets were anesthetized with 4% isoflurane, intubated, and mechanically ventilated. Femoral artery, femoral vein, and right carotid artery catheters were placed for continuous mean arterial blood pressure (MAP) recording (Grass-Telefactor, Astro-Med, West Warwick, RI), arterial blood gases, normal saline maintenance infusion at 4 ml/kg/hour, and cerebral blood flow determination using a previously described fluorescent microsphere technique (Eucker, et al., 2010). Ligation of a single carotid artery in piglets does not alter regional CBF over a wide range of CBF values due to extensive collateral cerebral circulation (Laptook, et al., 1983). Following catheter placement, isoflurane was reduced to 2.25-2.75% maintenance levels. A pre-injury blood gas and electrolyte sample was recorded (Nova Biomedical, Waltham, MA).

2.2. Non-impact rotational brain injury

Brain injury was induced using a well-characterized rotational acceleration device (Raghupathi and Margulies, 2002, Smith, et al., 2000) to impart a single rapid (12-20 msec), non-impact head rotation in either the horizontal, sagittal, or coronal plane relative to the cerebrum, centered at the mid-cervical spine (Figures 1A-C, respectively). Angular velocity was measured using an angular rate sensor (ATA, Inc.) attached to the linkage sidearm and captured using a PC-based data acquisition system at 10 kHz (LabView, National Instruments, Austin, TX).

The first group of piglets (HOR-HIGH, n=9) received a 90° horizontal rotation, with an average peak angular velocity (PAV) of 198 ± 12 rad/s (mean ± SD). The second group (COR, n=7) received a 90° coronal rotation, with an average peak angular velocity of 208 ± 11 rad/s. The third group (SAG, n=6) received a 60° sagittal rotation, with an average peak angular velocity of 166 ± 3 rad/s. The reduced angular excursion in this group was due to the limited range of motion of the piglet neck in the sagittal direction and resulted in a lower maximum angular velocity. To match the angular velocity loading conditions, a second horizontal group (HOR-LOW, n=6) received a 90° horizontal rotation at an average peak angular velocity of 168 ± 3 rad/s. The final group (SHAM, n=4) received all of the same pre-injury and post-injury procedures as the injured groups but did not undergo rotational injury.

Immediately prior to injury, anesthesia, supplemental oxygen, and mechanical ventilation were withdrawn, and the piglet was allowed to breathe spontaneously on room air. Following injury, the piglet was removed from the bite plate and supplemental oxygen was resumed, but the animal was allowed to continue breathing spontaneously. During this immediate post-injury period, the piglet was assessed for consciousness (reflexive withdrawal to pinch stimulus) and apnea (cessation of breathing or reduced respiratory effort resulting in SaO_2 <90%) every 30-60 sec. If apnea occurred, mechanical ventilation was immediately restarted. Once the pinch reflex was positive, both isoflurane anesthesia and mechanical ventilation were resumed.

Arterial blood gas samples were obtained at 5, 10, 15, 30, and 60 minutes post-injury and every subsequent hour for the duration of the study. Supplemental oxygen was titrated as needed to maintain pre-injury pO_2 levels (120-180 mmHg). Post-injury MAP was maintained within 10 mmHg of pre-injury MAP and above 40 mmHg by titrating the level of anesthesia and supplementing IV fluids with phenylephrine as needed, as this systemic vasoconstrictor has minimal effect on CBF (Strebel, et al., 1998). Between 15-30 min post-injury, an ICP transducer (Camino 110-4B, Integra, Plainsboro, NJ) was introduced into the subarachnoid space over the right parietal lobe, anterior to the coronal suture, in 29 of the 36 animals to monitor ICP post-injury.

At 6 hours post-injury, the piglet was sacrificed via pentobarbital overdose. The brain was perfusion-fixed using 0.9% saline followed by 10% neutral buffered formalin, removed, and post-fixed for >24 hours in 10% formalin for subsequent histological and fluorescent microsphere analysis. We focused our assessments on a 6 hours post-injury time point because while βAPP staining requires an 2-3 hours to turn positive in brain tissue after axonal injury (Hortobagyi, et al., 2007), ischemic changes can take up to 6 hrs to become visible on H&E (Petito, et al., 1987). This optimized time point allowed us to capture immediate changes in axonal injury (βAPP) and tissue ischemia (H&E), while minimizing the influence of later secondary sequelae that also contribute to both ischemia and axonal injury.

2.3. Cerebral blood flow measurements

CBF changes were measured before and after injury using a previously described fluorescent microsphere (FM) technique (Eucker, et al., 2010) in 7 animals from HOR-HIGH, 4 from COR, 4 from SAG, and 4 from HOR-LOW. Each animal received 1×10^6 FMs before injury and 2×10^6 FMs at 1 hr and 6 hrs post-injury, using a different randomized FM color (yellow-green, orange, or crimson) at each time point.

After each study, fixed brains were cut into 3 mm-thick coronal sections using a previously described piglet brain matrix (Eucker, et al., 2010). Every other section was reserved for histological assessment. Of the remaining sections, every other section was used for FM analysis (Figure 1D). This resulted in 4 total sections spaced evenly every 12 mm in the anterior-posterior direction, which could be subdivided into the following 9 regions: (1) right and (2) left frontal cerebrum including olfactory bulbs, (3) right and (4) left parietotemporal cerebrum including basal ganglia, (5) right and (6) left occipital cerebrum including hippocampus, and (7) midbrain-pons, (8) medulla, and (9) cerebellum. Global CBF was calculated from the total number of tissue microspheres in all right and left cerebral hemispheric regions (regions 1-6 above), excluding midbrain, brainstem, and cerebellum. Relative CBF measurements from each group were reported as mean ± standard error for each time point in each brain region.

2.4. Gross pathological and histopathological assessment

All gross and histopathological examinations were performed by a neuropathologist blinded to the injury group of the animal. Formalin-fixed injured and uninjured whole brains and subsequent 3 mm coronal sections were photographed and examined for gross pathology and subarachnoid hemorrhage. Following routine processing, tissue sections designated for histopathological examination (Figure 1D) were embedded in paraffin wax. From each section, a 6 μm thin slice was stained with haematoxylin & eosin (H&E), a second slice was stained with β-APP immunohistochemical marker, and all slices were lightly counterstained with Meyer's haematoxylin.

Slides were initially examined at a scanning power of 5-l0× magnification. Specific fields were further examined at 20-40× magnification. Microscopic assessment focused on the distributions of cellular injury and axonal damage. H&E sections were examined to document established infarcts, identified by changes in staining intensity, and ischemic neurons, characterized by cell shrinkage and eosinophilia (Figure 2). Axonal injury was assessed using β-APP immunohistochemistry, which marks disruption to axonal flow. For each animal, the distribution of axonal and neuronal injury were documented on the digital coronal section images.

Immunostaining density was scored in a semi-quantitative fashion that has been previously described (Williams, et al., 2001), in every field of every slice by a single observer to reduce inter-observer variation. Severity of ischemia in each brain was graded as either absent, mild, moderate, or severe in the manner of Graham et al. (Graham, et al., 1989). Cases were classified as severe if the lesions were diffuse, multifocal and large within arterial territories; moderate if the lesions were limited to the arterial boundary zones, singly or in combination with subtotal infarction in the distribution of the cerebral arteries, or if there were 3-5 subcortical lesions; mild if there were two or less subcortical lesions in the brain; and absent if there were no lesions present.

Brainstem injury was classified as absent, mild, moderate, or severe based on extents of both ischemic and white matter (βAPP) injuries, as shown in Figure 3. Subarachnoid hemorrhage (SAH) was classified as absent, mild (focal and patchy), moderate (solitary thick plaque obscuring brain, e.g. basal SAH, or multifocal patchy SAH over both hemispheres), or severe (extensive and obscuring) based on macroscopic and microscopic observations. Figure 4 shows representative images of each SAH classification.

For quantitative assessment of axonal injury and infarction, the two coronal sections flanking each FM analysis section (Figure 1D) were subdivided into matching regions for comparison of histopathology with regional CBF. Total tissue section area, area positive for βAPP, and area of infarction were quantified for each region from the photographic image documentation using ImageJ (NIH). These areas were used to calculate % axonal injury and % infarction for each region.

2.5. Statistical Analysis

Dunnett's tests were employed to determine whether each group differed from SHAM in terms of the following parameters: duration of unconsciousness, maximum phenylephrine dose administered, maximum change in fiO_2 levels, pO_2 and pCO_2 before and after injury, brainstem injury score, subarachnoid hemorrhage score, ischemia score, percentage of total tissue positive for βAPP, and percentage of total tissue infarction. One-way ANOVAs were used to compare gross pathological and histopathological findings between angular velocity-matched groups (HOR-HIGH vs COR and HOR-LOW vs SAG), and between HOR-HIGH and HOR-LOW. One-tailed Fisher's exact tests were used to determine whether each group differed from SHAM in terms of incidences of apnea, axonal injury, ischemic injury, and high ICP >20mmHg. Two-tailed Fisher's exact tests were used compare the same findings between velocity-load matched groups and between HOR groups described above.

Two-way ANOVAs were performed for each group to examine CBF changes across region and time post-injury. Two-way ANOVAs were performed for MAP, ICP, and cerebral perfusion pressure (CPP) differences across group and time post-injury. In addition, simple regression models were used to fit global CBF to CPP or MAP to determine whether CBF changes were related to pressure changes. Four-way repeated measures ANOVA were performed to compare regional CBF values over time between SHAM and each of the injured groups. Additional four-way ANOVAs were used to compare CBF changes between

velocity-load matched groups (HOR-HIGH vs COR and HOR-LOW vs SAG), and between HOR-HIGH and HOR-LOW.

To determine the effects of both decreased CBF and location within the brain on infarction and axonal injury in all animals, a separate multiple regression model for each injured group was fit to each of these pathological outcomes using CBF and brain region as parameters. When consistent models were found among directions, injured groups were combined, and the overall regression of the population was determined. Brain regions were redefined for regression analysis based on three spatial variables: anterior-posterior location, right-to-left location, and superior-inferior location. The tissue infarction and βAPP percentages were transformed to Gaussian distributed values by the arcsine transformation.

A linear regression model was used to fit global cerebral CBF vs. brainstem axonal injury for all injured animals, and the results were compared with regression models of global CBF and injury in randomly chosen brain regions to determine whether brainstem injury independently predicted overall CBF changes in the cerebrum. Separate correlations were used to compare global cerebral CBF with either ischemia score or total tissue % βAPP staining, and to compare ischemia score with total tissue % βAPP staining.

3. Results

Early physiological responses following injury differed by head rotation direction (Table 1). Post-injury unconsciousness times were significantly longer in SAG and HOR-LOW compared to SHAM. SAG and HOR-HIGH had significantly higher incidences of apnea compared to SHAM. In addition, ICP was significantly higher in SAG compared to SHAM across all times post-injury. In all injured groups, MAP typically increased transiently within the first 5 minutes post-injury, likely as a sympathetic response to injury, but by 10 minutes post-injury did not differ significantly from SHAM in any group. MAP decreased in SAG by 30 minutes post-injury relative to pre-injury, and significantly large doses of phenylephrine were required to return MAP to pre-injury levels (Table 1). Phenylephrine was required to raise post-injury MAP to pre-injury levels in several HOR-HIGH and COR animals as well, but the mean dose in these groups did not differ from SHAM. Therapeutic doses of phenylephrine were achieved by 1 hour post-injury in all animals, such that CPP did not differ in any group from pre-injury or from SHAM for the remainder of the study.

CBF decreased significantly across all regions from pre-injury to 1 hr post-injury in every group except SHAM (Figure 5A). Further significant decreases were seen from 1 hr to 6 hrs post-injury in HOR-HIGH and COR. There were no significant regional variations in CBF in any group at any time. CBF decreases at 1 hr and 6 hrs post-injury were significantly different from SHAM in SAG, but not in HOR-HIGH, HOR-LOW, or COR. Furthermore, CBF did not differ significantly at any time point between HOR-HIGH and COR, between HOR-LOW and SAG, or between HOR-HIGH and HOR-LOW. CPP did not differ significantly from SHAM in any injured group for these animals, and regression analysis showed no correlation between CPP or MAP changes and CBF. There were no significant differences in pO_2 or pCO_2 between SHAM and any of the injured groups that would explain the sustained post-injury decreases in CBF. In addition, regression analysis showed no relationship between early global post-injury CBF reductions and brainstem injury ($p = 0.07$).

Early gross pathological findings differed by head rotation direction (Table 2). SAH score was significantly greater than SHAM in HOR-HIGH and SAG. Early ischemia score was significantly greater than SHAM in SAG only. Brainstem injury score did not differ significantly from SHAM in any group. In addition, HOR-HIGH had significantly higher

SAH, ischemia, and brainstem injury scores than COR; SAG had significantly higher SAH and ischemia scores than HOR-LOW; and HOR-HIGH had significantly higher SAH and brainstem injury scores than HOR-LOW.

Early histopathological findings also differed by injury direction (Figures 5B and 6). Total axonal injury by βAPP staining was significantly greater than SHAM in HOR-HIGH, HOR-LOW, and SAG. HOR-HIGH had significantly more axonal injury than COR and HOR-LOW. However, extent of axonal injury did not differ between HOR-LOW and SAG. The percentages of total or regional tissue infarction did not differ significantly between SHAM and any injured group, or among any of the injured groups, likely due to the small size of infarcted regions in affected animals. However, the incidence of ischemic injury did differ by direction (Table 3, Figure 7), occurring more often in SAG than in SHAM and more often in HOR-HIGH than in COR.

The incidences of other pathological findings also differed by injury direction (Table 3). SAH occurred significantly more often in HOR-HIGH, HOR-LOW, and SAG than in SHAM, and axonal injury occurred more often in HOR-HIGH, HOR-LOW, and SAG than in SHAM. In addition, HOR-HIGH had significantly higher incidences of SAH, axonal injury, and brainstem injury compared to COR, whereas SAG did not differ from HOR-LOW in the incidences of any of these findings. HOR-HIGH only differed from HOR-LOW in the incidence of brainstem injury.

Multiple regression analysis revealed greater axonal injury in more anterior regions of the brain in every injury group, but no relationship with 1 hr post-injury CBF. This suggests that certain regions of the brain are more susceptible to axonal injury regardless of rotation direction, and that decreased CBF was not the primary factor in the pathogenesis of this injury. Significant correlation between axonal injury and decreased 6 hr CBF was identified in SAG only. This may be due to local CBF reductions over time in response to reduced metabolic demand in injured tissues in this animal group.

Interestingly, in HOR-HIGH and HOR-LOW, greater regional tissue infarction occurred in more anterior brain regions but did not correlate with CBF. In the SAG group, regional infarction did not correlate with 1 hr post-injury CBF, but did correlate with 6 hr CBF, which may again reflect local CBF reductions in response to reduced metabolic demand. No infarction was observed in the COR group. Taken together, these findings suggest that the mechanisms involved in tissue infarction likely differ by rotation direction.

Total brain % βAPP staining and ischemia score were highly correlated ($p < 0.01$, Figure 8A), but neither correlated with global CBF. In addition, regional % βAPP staining and regional % tissue infarction were significantly correlated, such that regions with larger amounts of tissue infarction also had larger amounts of axonal injury (Figure 8B). However, while all 14 animals with ischemia had axonal injury, not all 26 animals with axonal injury had ischemia. Large amounts of βAPP staining occurred in both ischemic and non-ischemic brains, but ischemic injury occurred only in animals that had large amounts of βAPP staining.

These data suggest that while graded axonal injury can occur under varying conditions, early ischemic injury only occurs under conditions in which larger amounts of axonal injury are observed. The extent of individual regions of early ischemic changes and infarction are frequently small, do not correlate with global CBF, and do not follow a consistent vascular or watershed distribution, suggesting local metabolic derangement or a thrombotic mechanism for these injuries.

4. Discussion

Little is known about the effects of altering direction of head rotation on outcomes following TBI, particularly in the pediatric population. Our study of non-impact rotational head injury in neonatal piglets demonstrates direction-dependent differences in early neurological and pathological outcomes. Coronal rotation produced few signs of neurological disability and little to no gross or histological pathological findings. Both horizontal and sagittal rotations produced worse neurological derangements, including longer durations of unconsciousness and higher incidences of apnea and hypotension. In addition, axonal injury and SAH were present to varying extents in nearly every animal in these two groups, and ischemia and infarction were common early post-injury.

In adult pigs, the physiological data are similar but the pathological findings differ somewhat from neonatal piglets (Smith, et al., 2000). In adult pigs, only the brainstem had greater axonal injury after horizontal compared with coronal rotation (Smith, et al., 2000), whereas in our pediatric animals all brain regions had greater injury. Likewise, SAH severity did not differ between these two directions in adult pigs (Smith, et al., 2000), whereas more extensive SAH was produced by horizontal than by coronal rotation in neonatal piglets. The decreased susceptibility of the developing brain to pathological changes following coronal rotation may be due to its smaller size and incomplete myelination. Since coronal rotations have a much smaller radius of rotation than either horizontal or sagittal rotations, inertial differences in this direction are more affected by brain mass (moment of inertia = mass × radius^2). In addition, reduced myelination decreases the stiffness of white matter tracts compared to those of adults (Prange and Margulies, 2002) and makes them less likely to stretch under similar stresses.

Directional comparisons performed in adult primates focused on brainstem injury and demonstrated more severe lesions and clinical sequelae after coronal than after horizontal rotations (Gennarelli, et al., 1982, Gennarelli, et al., 1987). Because the brain of the bipedal primate has a different brainstem orientation relative to the cerebrum than does the quadripedal piglet, we hypothesize that the brainstem loading conditions of coronal rotations in the primate more closely match those of horizontal rotations in the piglet. Thus, the direction-dependent differences in brainstem injuries between horizontal and coronal rotations are consistent between piglets and adult primates.

By contrast, sagittal rotations produced only mild brainstem injury in the primate (Gennarelli, et al., 1987), differing from the severe injuries observed in piglets. This may again be due to differences in brainstem anatomy between the species. The piglet brainstem sits in close proximity to the base of the skull ventral to the cerebrum and cerebellum (Sisson and Grossman, 1975), leaving it relatively unshielded from the higher stresses that are posited to occur near the brain-skull boundary (Ommaya, 1985). The primate brainstem, however, is separated from the skull in the sagittal plane by the cerebrospinal fluid-filled pontine cistern, which may provide sufficient cushioning to dampen those same stresses. Another difference between the study groups is that sagittal rotations in our piglets were performed from neck flexion to extension, whereas those in primates were performed from neck extension to flexion. Since the cerebellum is located dorsal to the brainstem, it would be expected to receive most of the stresses during neck flexion, again protecting the brainstem during sagittal injury in the primate.

4.1. Mechanisms of direction-dependent axonal injury

Trauma is thought to cause axonal injury through a mechanism known as delayed secondary axotomy, in which a functional disturbance of the axon leads to localized inhibition of axonal transport at nodes of Ranvier, visible as axonal swellings and bulbs via

immunohistochemistry, and the eventual separation of the axon at the node hours to days later (Maxwell, et al., 1997). βAPP immunohistochemical evidence of these processes is almost always observed in fatal TBI (Gentleman, et al., 1995).

There is much debate as to whether the functional disturbance is of mechanical or metabolic origin. Diffuse axonal injury has historically been attributed to strain-related mechanisms (Gennarelli, et al., 1982, Margulies, et al., 1990, Ommaya, 1985). Physical models of the primate skull with a gelatin representation of the brain have demonstrated close correspondence between regional shear strain and regions of axonal injury observed in primates undergoing rotational TBI (Margulies, et al., 1990).

The high incidence of ischemic injury in fatal TBI raises the possibility that hypoxia-ischemia is the primary mechanism by which traumatic axonal injury occurs (Geddes, et al., 2001, Graham, et al., 1989). However, the severity and extent of axonal βAPP staining observed in the setting of non-traumatic hypoxic-ischemic injury are significantly less than observed in TBI (Dolinak, et al., 2000), and others have demonstrated a distinct absence of axonal βAPP staining following hypoxic-ischemic injury in both infants and neonatal animals (Baiden-Amissah, et al., 1998).

Our study is uniquely positioned to address this issue. We have directly imparted a measured and well-characterized mechanical insult, and we compared the relationship between early ischemic mechanisms or mechanical mechanisms and the development of axonal injury. Our data demonstrated greater axonal injury under higher mechanical loading conditions, but not greater ischemia or CBF reductions. While we did find a correlation between total axonal injury and total ischemia, we found no correlation between regional axonal injury and regional CBF, and ischemia did not occur in all animals with axonal injury. Early ischemic injury occurred predominantly in animals with more extensive axonal injury, and the spatial extent of ischemia was generally less than that of axonal injury. We conclude that early post-injury ischemia is most likely an epiphenomenon of severe inertial loading and not the primary causal factor in the development of axonal injury in our animals.

Our finding of greater axonal injury in the frontal and temporal regions following both horizontal and sagittal rotations suggests these regions are particularly vulnerable to trauma. A recent study of patients with mild TBI used diffusion tensor imaging and region-of-interest analysis to quantify the spatial distribution of microstructural white matter injury in the cerebral hemispheres (Niogi, et al., 2008). This study revealed that axonal injury occurred most often in the frontal and temporal poles, consistent with our findings. Anterior brain regions are also the most common sites of contrecoup contusion in TBI patients, regardless of head impact site (Tasker, 2006). This pattern has been hypothesized to be caused by larger strains in these regions, due to the irregular brain and skull geometries around the frontal and temporal lobes as well as the greater distance from the center of rotation at the cervical spine (Margulies, et al., 1990, Tasker, 2006). Since contrecoup contusions occur primarily as a result of head acceleration after impact and are typically distal to the impact site (Adams, et al., 1985), we postulate that similar mechanical mechanisms are responsible for both contrecoup and rotationally-induced axonal injury.

4.2. Mechanisms of direction-dependent cerebral blood flow reductions

To our knowledge, direction-dependent changes in CBF immediately following rotational head injury have never before been characterized. Widespread CBF reductions relative to pre-injury levels were observed at both 1 hr and 6 hrs post-injury in every injury group, with no significant regional CBF variation in any group. The lack of regional CBF heterogeneity is likely due to the diffuse nature of rotational brain injuries (Gennarelli, et al., 1982, Raghupathi and Margulies, 2002, Smith, et al., 2000). Greater regional CBF heterogeneity

occurs in patients with more focal lesions, such as contusions (Chieregato, et al., 2004), whereas patients with diffuse TBI have more global reductions in CBF with little regional variability (Adelson, et al., 1997, Shiina, et al., 1998). Because the primary resistance vessels in the brain are the small arterioles, which account for roughly 50-55% of CBF regulation (Golding, et al., 1999), we postulate that the observed global CBF reductions are due to generalized vasoconstriction of cerebral arterioles.

However, we observed direction-dependent differences in both the magnitude and time course of these CBF reductions, suggesting that global vasoconstriction may be modulated by regional tissue strain during injury. This idea is supported by studies showing that longitudinal stretch of isolated canine and rabbit cerebral arterioles causes a rapid vasoconstrictive response (Tanaka, et al., 1998). Furthermore, ultrastructural observations following stretch injury of guinea pig optic nerves (Maxwell, et al., 1991) or head injury in baboons (Maxwell, et al., 1988) demonstrate widespread microvascular endothelial dysfunction in bilateral optic nerves or cerebral white matter, respectively. The mechanism of stretch-induced vasoconstriction may be myogenic or mediated by alterations in levels of vasoactive biochemical signals, such as increases in endothelial-derived vasconstrictors, including endothelin, thromboxane, and opoids and/or decreases in both production of and response to vasodilatory signals (Armstead, 2005, Golding, et al., 1999).

CBF reductions may also occur secondary to decreased tissue metabolism (Sharples, et al., 1995). Coupling of CBF with metabolic demand is suggested by the greater correlation of CBF with both axonal injury and infarction in SAG at 6 hrs compared with 1 hr post-injury. However, the head rotation direction-dependent effects of rotational injury on cerebral metabolic rate are unknown.

The direction-dependent differences in CBF may be secondary to functional brainstem injury after sagittal rotation. SAG had a high incidence of apnea and required significantly higher doses of phenylephrine to maintain normal MAP, indicating greater brainstem dysfunction. While brainstem regulation of CBF is not well understood, abnormal increases or decreases in the activity of these regulatory pathways may lead to post-traumatic microvascular dysfunction. Dysfunction may extend into the upper cervical region where the sympathetic nuclei are located, leading to an abnormal upregulation of the sympathetic vasoconstrictive response (Shibata, et al., 1993).

Alternatively, the greater CBF reductions in SAG may be due to higher strains at the base of the brain during rotation in this direction, causing greater stretch of the carotid arteries as they enter the cranium. The greater degree of brainstem dysfunction in SAG may also be due to these higher strains and may be an epiphenomenon, rather than a causal factor, of the CBF reductions. While isolated large artery constriction normally has minimal effects on CBF due to microvascular autoregulation, in the setting of trauma-induced endothelial dysfunction large artery constriction may result in profound decreases in global CBF. The absence of this response in the HOR group is likely because only one carotid artery is stretched during rotation in this direction, and an intact Circle of Willis re-distributes blood from the patent vessel to the entire brain (Sisson and Grossman, 1975).

4.3. Mechanisms of direction-dependent ischemic injury

We found a high incidence of early ischemic injury, 47% of all injured animals, consistent with the high incidence of hypoxic-ischemic injuries seen in human pediatric and adult TBI fatalities (Geddes, et al., 2001, Graham, et al., 1989). However, neither ischemia score nor regional infarction correlated with global or regional CBF, respectively. Interestingly, the incidence and severity of ischemic injury differed by head rotation direction, with SAG producing the worst, HOR-HIGH and HOR-LOW producing intermediate amounts, and

COR producing no ischemic injury or infarct. Early infarction never occurred in the absence of axonal injury and was more frequent in regions with more extensive axonal injury. Together, these results suggest that early ischemic injuries following trauma are tissue strain-dependent. This hypothesis is further supported by a study in primates, which found a strong inverse power-law relationship between physical model-predicted maximum principal strains and regional brain tissue ATP levels, where lower ATP levels were used indicate reduced oxygen metabolism (Thibault, et al., 1991).

Apnea is a frequent sequela of TBI in children and adults and may lead to hypoxic-ischemic brain injury (Geddes, et al., 2001, Johnson, et al., 1995). While we also observed a high incidence of apnea in our animals, mechanical ventilatory support was immediately initiated for blood oxygen saturations <90%. Thus, the ischemic injury observed in our animals is unlikely to be due to systemic hypoxia.

Interestingly, although there was no significant regional CBF variation in any injury group, tissue ischemia and infarction were much more heterogeneously distributed. Regions of ischemia and infarction were typically small, usually <10% of the area of a single brain region, but multi-focal in both location and vascular territory. One possible reason is that localized regions of increased tissue metabolic rate and/or decreased CBF are smaller than the resolution of our FM measurements. Another possibility is that the local ischemic threshold is altered secondary to changes in local tissue metabolic rate (Sharples, et al., 1995). The final possibility, and the most common cause of infarction, is endothelial injury leading to thrombus formation and localized vascular occlusion (Cotran, et al., 1999).

5. Conclusions

Early injury outcomes including regional cerebral blood flow and regional tissue pathology differ by head rotation direction following non-impact inertial injury. Sagittal rotations resulted in the worst physiological dysfunction and cerebral blood flow reductions, while both sagittal and horizontal rotations produced the greatest degrees of tissue pathology. Coronal rotations did not result in any significant physiological or pathological sequelae. Regional axonal injury and infarction did not correlate with regional cerebral blood flow. The direction-dependent differences in immediate post-injury outcomes are likely due to differences in mechanical loading (e.g. tissue strain) produced during head rotation.

Acknowledgments

The authors would like to thank Dr. Nicole Ibrahim, Dr. Brittany Coats, Rahul Natesh, Sarah Casey, and Alison Agres for their valuable technical expertise. This research was funded by the American Heart Association and NIH R01 NS39679.

Sources of support: NIH R01 NS39679, American Heart Association, Whitaker Foundation

References

1. Adams JH, Doyle D, Graham DI, Lawrence AE, McLellan DR, Gennarelli TA, Pastuszko M, Sakamoto T. The contusion index: a reappraisal in human and experimental non-missile head injury. Neuropathol Appl Neurobiol 1985;11:299–308. [PubMed: 4058674]
2. Adelson PD, Clyde B, Kochanek PM, Wisniewski SR, Marion DW, Yonas H. Cerebrovascular response in infants and young children following severe traumatic brain injury: a preliminary report. Pediatr Neurosurg 1997;26:200–207. [PubMed: 9436831]
3. Arbogast KB, Margulies SS, Christian CW. Initial neurologic presentation in young children sustaining inflicted and unintentional fatal head injuries. Pediatrics 2005;116:180–184. [PubMed: 15995050]
4. Armstead WM. Age and cerebral circulation. Pathophysiology 2005;12:5–15. [PubMed: 15927820]

5. Baiden-Amissah K, Joashi U, Blumberg R, Mehmet H, Edwards AD, Cox PM. Expression of amyloid precursor protein (beta-APP) in the neonatal brain following hypoxic ischaemic injury. Neuropathol Appl Neurobiol 1998;24:346–352. [PubMed: 9821164]
6. Bayir H, Kochanek PM, Clark RS. Traumatic brain injury in infants and children: mechanisms of secondary damage and treatment in the intensive care unit. Crit Care Clin 2003;19:529–549. [PubMed: 12848319]
7. Chieregato A, Fainardi E, Servadei F, Tanfani A, Pugliese G, Pascarella R, Targa L. Centrifugal distribution of regional cerebral blood flow and its time course in traumatic intracerebral hematomas. J Neurotrauma 2004;21:655–666. [PubMed: 15253794]
8. Cotran, RS.; Kumar, V.; Collins, T.; Robbins, SL. Robbins pathologic basis of disease. W. B. Saunders; 1999.
9. Dolinak D, Smith C, Graham DI. Global hypoxia per se is an unusual cause of axonal injury. Acta Neuropathol (Berl) 2000;100:553–560. [PubMed: 11045678]
10. Duhaime AC, Alario AJ, Lewander WJ, Schut L, Sutton LN, Seidl TS, Nudelman S, Budenz D, Hertle R, Tsiaras W, et al. Head injury in very young children: mechanisms, injury types, and ophthalmologic findings in 100 hospitalized patients younger than 2 years of age. Pediatrics 1992;90:179–185. [PubMed: 1641278]
11. Eucker SA, Hoffman BD, Natesh R, Ralston J, Armstead WM, Margulies SS. Development of a fluorescent microsphere technique for rapid histological determination of cerebral blood flow. Brain Res 2010;1326:128–134. [PubMed: 20193669]
12. Geddes JF, Hackshaw AK, Vowles GH, Nickols CD, Whitwell HL. Neuropathology of inflicted head injury in children. I. Patterns of brain damage. Brain 2001;124:1290–1298. [PubMed: 11408324]
13. Gennarelli TA, Thibault LE, Adams JH, Graham DI, Thompson CJ, Marcincin RP. Diffuse axonal injury and traumatic coma in the primate. Ann Neurol 1982;12:564–574. [PubMed: 7159060]
14. Gennarelli, TA.; Thibault, LE.; Tomei, G.; Wiser, R.; Graham, D.; Adams, J. Directional Dependence of Axonal Brain Injury Due to Centroidal and Non-Centroidal Acceleration. STAPP Car Crash Conference; New Orleans, LA. 1987. p. 49-53.
15. Gentleman SM, Roberts GW, Gennarelli TA, Maxwell WL, Adams JH, Kerr S, Graham DI. Axonal injury: a universal consequence of fatal closed head injury? Acta Neuropathol (Berl) 1995;89:537–543. [PubMed: 7676809]
16. Golding EM, Robertson CS, Bryan RM Jr. The consequences of traumatic brain injury on cerebral blood flow and autoregulation: a review. Clin Exp Hypertens 1999;21:299–332. [PubMed: 10369378]
17. Graham DI, Ford I, Adams JH, Doyle D, Teasdale GM, Lawrence AE, McLellan DR. Ischaemic brain damage is still common in fatal non-missile head injury. J Neurol Neurosurg Psychiatry 1989;52:346–350. [PubMed: 2926419]
18. Gruskin KD, Schutzman SA. Head trauma in children younger than 2 years: are there predictors for complications? Arch Pediatr Adolesc Med 1999;153:15–20. [PubMed: 9894994]
19. Hortobagyi T, Wise S, Hunt N, Cary N, Djurovic V, Fegan-Earl A, Shorrock K, Rouse D, Al-Sarraj S. Traumatic axonal damage in the brain can be detected using beta-APP immunohistochemistry within 35 min after head injury to human adults. Neuropathol Appl Neurobiol 2007;33:226–237. [PubMed: 17359363]
20. Johnson DL, Boal D, Baule R. Role of apnea in nonaccidental head injury. Pediatr Neurosurg 1995;23:305–310. [PubMed: 8743999]
21. Kochanek PM, Clark RS, Ruppel RA, Adelson PD, Bell MJ, Whalen MJ, Robertson CL, Satchell MA, Seidberg NA, Marion DW, Jenkins LW. Biochemical, cellular, and molecular mechanisms in the evolution of secondary damage after severe traumatic brain injury in infants and children: Lessons learned from the bedside. Pediatr Crit Care Med 2000;1:4–19. [PubMed: 12813280]
22. Langlois, JA.; Rutland-Brown, W.; Thomas, KE. Traumatic brain injury in the United States: emergency department visits, hospitalizations, and deaths. Centers for Disease Control and Prevention, National Center for Injury Prevention and Control. Centers for Disease Control and Prevention, National Center for Injury Prevention and Control; Atlanta, GA: 2004.

23. Laptook AR, Stonestreet BS, Oh W. The effect of carotid artery ligation on brain blood flow in newborn piglets. Brain Res 1983;276:51–54. [PubMed: 6627001]
24. Margulies SS, Thibault LE, Gennarelli TA. Physical model simulations of brain injury in the primate. J Biomech 1990;23:823–836. [PubMed: 2384494]
25. Maxwell WL, Irvine A, Adams JH, Graham DI, Gennarelli TA. Response of cerebral microvasculature to brain injury. J Pathol 1988;155:327–335. [PubMed: 3171774]
26. Maxwell WL, Irvine A, Watt C, Graham DI, Adams JH, Gennarelli TA. The microvascular response to stretch injury in the adult guinea pig visual system. J Neurotrauma 1991;8:271–279. [PubMed: 1803035]
27. Maxwell WL, Povlishock JT, Graham DL. A mechanistic analysis of nondisruptive axonal injury: a review. J Neurotrauma 1997;14:419–440. [PubMed: 9257661]
28. Niogi SN, Mukherjee P, Ghajar J, Johnson C, Kolster RA, Sarkar R, Lee H, Meeker M, Zimmerman RD, Manley GT, McCandliss BD. Extent of microstructural white matter injury in postconcussive syndrome correlates with impaired cognitive reaction time: a 3T diffusion tensor imaging study of mild traumatic brain injury. AJNR Am J Neuroradiol 2008;29:967–973. [PubMed: 18272556]
29. Ommaya, AK. Biomechanics of Head Injury: Experimental Aspects. In: Nahum, AM.; Melvin, J., editors. The Biomechanics of Trauma. Appleton-Century-Crofts; Norwalk, CT: 1985. p. 245-269.
30. Petito CK, Feldmann E, Pulsinelli WA, Plum F. Delayed hippocampal damage in humans following cardiorespiratory arrest. Neurology 1987;37:1281–1286. [PubMed: 3614648]
31. Prange MT, Margulies SS. Regional, directional, and age-dependent properties of the brain undergoing large deformation. J Biomech Eng 2002;124:244–252. [PubMed: 12002135]
32. Raghupathi R, Margulies SS. Traumatic axonal injury after closed head injury in the neonatal pig. J Neurotrauma 2002;19:843–853. [PubMed: 12184854]
33. Sharples PM, Stuart AG, Matthews DS, Aynsley-Green A, Eyre JA. Cerebral blood flow and metabolism in children with severe head injury. Part 1: Relation to age, Glasgow coma score, outcome, intracranial pressure, and time after injury. J Neurol Neurosurg Psychiatry 1995;58:145–152. [PubMed: 7876842]
34. Shibata M, Einhaus S, Schweitzer JB, Zuckerman S, Leffler CW. Cerebral blood flow decreased by adrenergic stimulation of cerebral vessels in anesthetized newborn pigs with traumatic brain injury. J Neurosurg 1993;79:696–704. [PubMed: 8105043]
35. Shiina G, Onuma T, Kameyama M, Shimosegawa Y, Ishii K, Shirane R, Yoshimoto T. Sequential assessment of cerebral blood flow in diffuse brain injury by 123I-iodoamphetamine single-photon emission CT. AJNR Am J Neuroradiol 1998;19:297–302. [PubMed: 9504482]
36. Sisson, S.; Grossman, JD. The Anatomy of the Domestic Animals. W. B. Saunders; 1975.
37. Smith DH, Nonaka M, Miller R, Leoni M, Chen XH, Alsop D, Meaney DF. Immediate coma following inertial brain injury dependent on axonal damage in the brainstem. J Neurosurg 2000;93:315–322. [PubMed: 10930019]
38. Strebel SP, Kindler C, Bissonnette B, Tschaler G, Deanovic D. The impact of systemic vasoconstrictors on the cerebral circulation of anesthetized patients. Anesthesiology 1998;89:67–72. [PubMed: 9667295]
39. Tanaka Y, Shigenobu K, Nakayama K. Inhibitory actions of various vasorelaxants on the myogenic contraction induced by quick stretch studied in canine cerebral artery. European Journal of Pharmacology 1998;356:225–230. [PubMed: 9774253]
40. Tasker RC. Changes in white matter late after severe traumatic brain injury in childhood. Dev Neurosci 2006;28:302–308. [PubMed: 16943653]
41. Thibault, LE.; Boock, RJ.; Gennarelli, TA. Strain dependent ischemia in brain tissue as a function of inertial loading of the head. IRCOBI; Berlin: 1991. p. 101-113.
42. Williams S, Raghupathi R, MacKinnon MA, McIntosh TK, Saatman KE, Graham DI. In situ DNA fragmentation occurs in white matter up to 12 months after head injury in man. Acta Neuropathol (Berl) 2001;102:581–590. [PubMed: 11761718]

Abbreviations

CBF	cerebral blood flow
CPP	cerebral perfusion pressure
FM	fluorescent microsphere
ICP	intracranial pressure
MAP	mean arterial blood pressure
SAH	subarachnoid hemorrhage
SaO_2	arterial oxygen saturation
TBI	traumatic brain injury

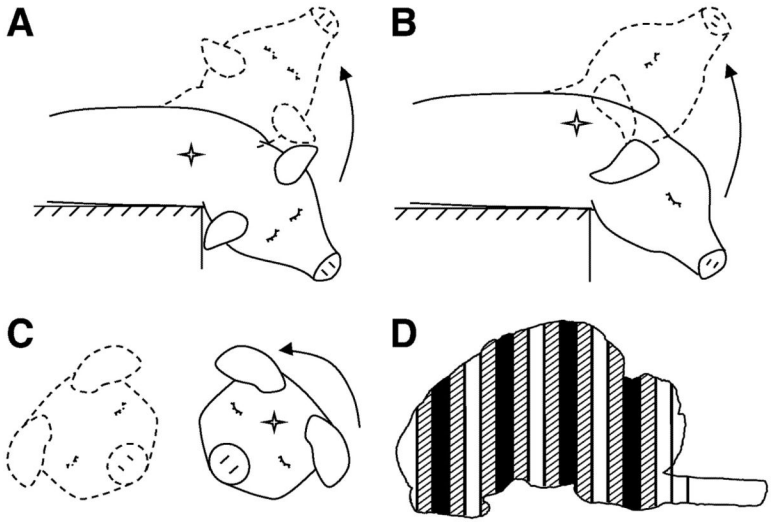

Figure 1.

Schematic of piglet head rotation in the (A) Sagittal, (B) Horizontal, and (C) Coronal directions. The direction of head motion is indicated by an arrow. The center of rotation is indicated by a star (✧). Solid lines represent head position before rotation, and dotted lines represent position after rotation. (D) Diagram of sliced coronal brain sections. Solid sections (■) were used for FM analysis. Hatched sections (▨) were used for histological analysis.

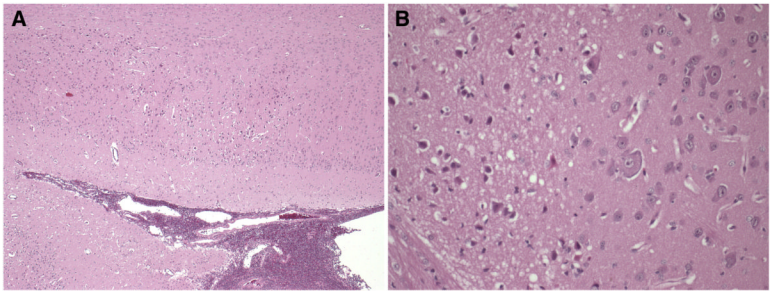

Figure 2.
H&E section at low (4×, A) and high (20×, B) power, demonstrating infarcts, identified by changes in staining intensity, and ischemic neurons, characterized by cell shrinkage and eosinophilia.

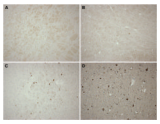

Figure 3.
Representative images demonstrating the range of brainstem injury scores, based on extents of both ischemic and white matter (βAPP) injuries: (A) absent, (B) mild, (C) moderate, and (D) severe.

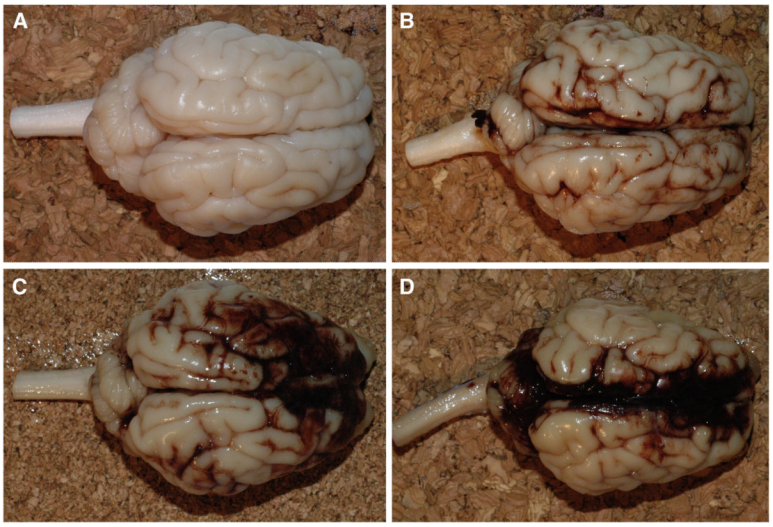

Figure 4.

Representative images demonstrating the range of subarachnoid hemorrhage (SAH) scores based on macroscopic and microscopic observations: (A) absent, (B) mild, focal and patchy, (C) moderate, solitary thick plaque obscuring brain, e.g. basal SAH, or multifocal patchy SAH over both hemispheres, and (D) severe extensive and obscuring.

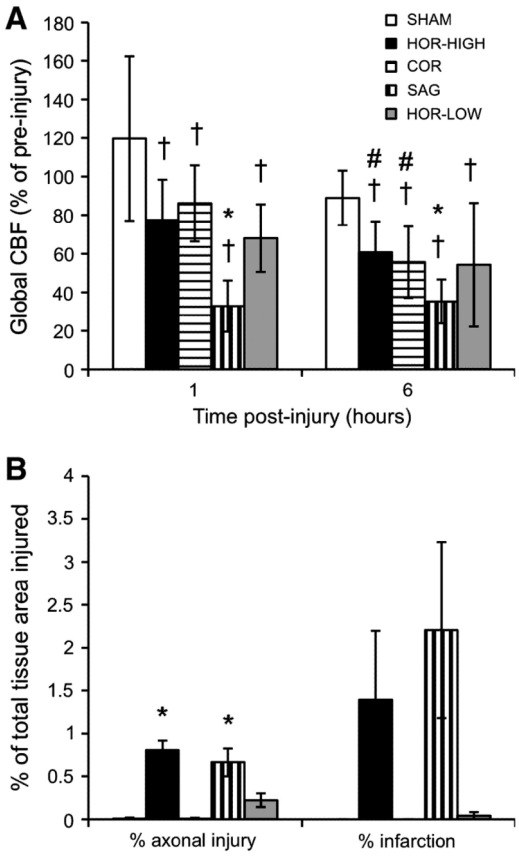

Figure 5.

(A) Summary of CBF changes over time (mean ± SEM). (B) Summary of histopathological findings (mean ± SEM). *indicates significant difference from SHAM. †indicates significant difference from pre-injury CBF. #indicates significant difference from 1 hr post-injury.

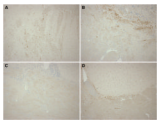

Figure 6.
Representative images demonstrating axonal injury findings in (A) HOR-HIGH, (B) SAG, (C) COR, and (D) HOR-LOW injury groups. Note the extensive positive βAPP staining in (A) HOR-HIGH and (B) SAG, the minimal staining in (D) HOR-LOW, and the lack of staining in (C) COR.

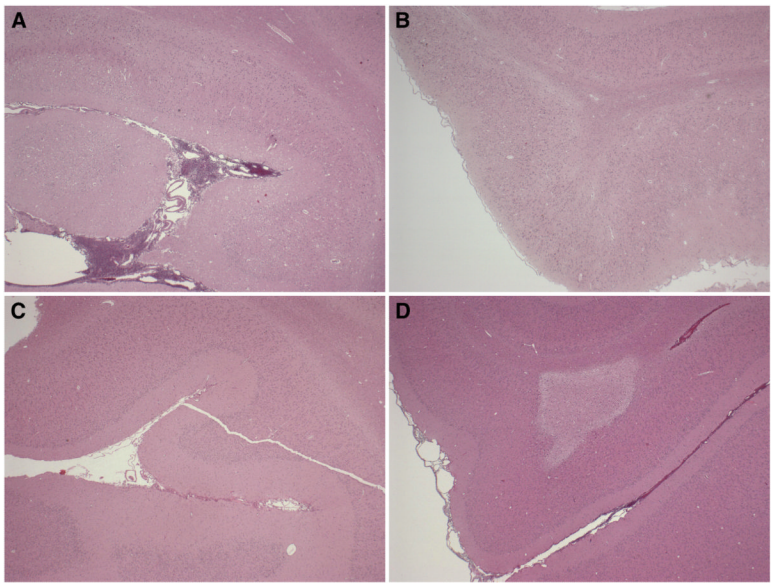

Figure 7.
Representative images demonstrating immediate post-injury areas of infarction in (A) HOR-HIGH, (B) SAG, (C) COR, and (D) HOR-LOW injury groups. Note the extensive areas of pale infarcted tissue in (A) HOR-HIGH and (B) SAG, the small area of infarct in (D) HOR-LOW, and the lack of infarcted tissue in (C) COR.

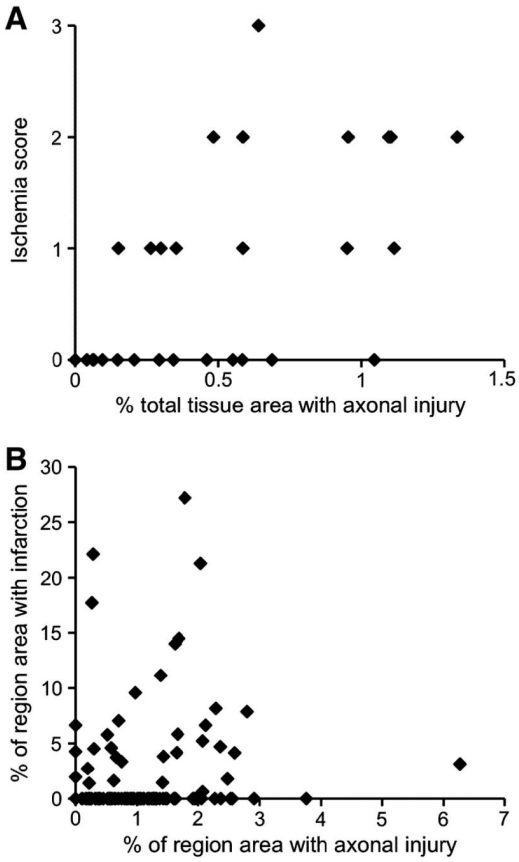

Figure 8.
(A) Comparison of ischemia score with % total axonal injury. (B) Correlation between % regional tissue infarction with % regional axonal injury for all brain regions in all injured animals ($p < 0.05$).

Table 1

Summary of injury loads and clinical findings for each injury group and SHAM.

Group	n	Angular velocity (rad/s, ± SD)	Unconsciousness time (min, ± SEM)	% Apneic	Peak PE dose (mcg/kg/min, ± SEM)
SHAM	4	0	1.7 ± 0.8	0	0
HOR-HIGH	9	198 ± 12	7.1 ± 1.8	67*	15.6 ± 8.0
COR	7	208 ± 11	3.7 ± 1.1	14	8.6 ± 5.9
SAG	6	166 ± 3	11.0 ± 1.9*	100*	138.3 ± 36.6*
HOR-LOW	7	168 ± 3	8.9 ± 1.3*	0	0

* indicates significant difference from SHAM.

Table 2

Summary of gross pathology scores for each group (mean ± SEM).

Group	SAH score	Ischemia score	BS score
SHAM	0	0	0
HOR-HIGH	1.9 ± 0.2*	1.00 ± 0.37	0.89 ± 0.31
COR	0.3 ± 0.2	0	0
SAG	2.2 ± 0.4*	1.33 ± 0.33*	0.83 ± 0.40
HOR-LOW	1.0 ± 0.3	0.33 ± 0.21	0

* indicates significant difference from SHAM. Subarachnoid hemorrhage (SAH) score = graded from 0 (absent) to 3 (extensive and obscuring). Ischemia score = graded 0 (absent) to 3 (diffuse, multifocal, and large lesions). Brainstem (BS) score = graded from 0 (absent) to 3 (multifocal prominent staining) based on extent of both ischemic and white matter (β-APP) injury.

Table 3

Incidences of axonal injury, ischemia, brainstem injury, and subarachnoid hemorrhage for each injury group and SHAM (% of group).

Group	n	Axonal injury by β-APP	Ischemic injury	Brainstem injury	Subarachnoid hemorrhage
SHAM	4	25	0	0	0
HOR-HIGH	9	100*	56	56	100*
COR	7	14	0	0	29
SAG	6	100*	83*	50	100*
HOR-LOW	6	100*	33	0	83*

* indicates significant difference from SHAM.